Regular paper

Title: Identification and characterization of extracellular GH3 β-glucosidase from the pink snow mold fungus, *Microdochium nivale*

Author information:

Tomoya Ota,[1] Wataru Saburi,[1] Linda Elizabeth Jewell,[2] Tom Hsiang,[3] Ryozo Imai,[4] and Haruhide Mori[1†]

[1]*Research Faculty of Agriculture, Hokkaido University (Kita 9 Nishi 9, Sapporo 060-8589, Japan)*

[2]*Agriculture and Agri-Food Canada (204 Brookfield Road, St. John's, Newfoundland and Labrador A1E 6J5)*

[3] *School of Environmental Sciences, University of Guelph (Guelph, ON N1G 2W1, Canada)*

[4] *Institute of Agrobiological Sciences, National Agriculture and Food Research Organization (3-1-3 Kannondai, Tsukuba, Ibaraki 305-8604, Japan)*

[†]Corresponding Author (Postal address: Research Faculty of Agriculture, Hokkaido University, Kita 9 Nishi 9, Sapporo 060-8589, Japan; E-mail address: hmori@agr.hokudai.ac.jp)

Running head: *Microdochium nivale* GH3 β-glucosidase

Abstract:

Glycoside hydrolase family 3 (GH3) β-glucosidase exists in many filamentous fungi. In phytopathogenic fungi, it is involved in fungal growth and pathogenicity. *Microdochium nivale* is a severe phytopathogenic fungus of grasses and cereals and is the causal agent of pink snow mold, but its β-glucosidase has not been identified. In this study, a GH3 β-glucosidase of *M. nivale* (MnBG3A) was identified and characterized. Among various *p*-nitrophenyl β-glycosides, MnBG3A showed activity on D-glucoside (pNP-Glc) and slight activity on D-xyloside. In the pNP-Glc hydrolysis, substrate inhibition occurred (K_{is} = 1.6 mM), and D-glucose caused competitive inhibition (K_i = 0.5 mM). MnBG3A acted on β-glucobioses with β1-3, -6, -4, and -2 linkages, in descending order of k_{cat}/K_m. In contrast, the regioselectivity for newly formed products was limited to β1-6 linkage. MnBG3A has similar features to those of β-glucosidases from *Aspergillus* spp., but higher sensitivity to inhibitory effects.

Key words:

Microdochium nivale, β-glucosidase, glycoside hydrolase family 3, substrate specificity, transglucosylation

INTRODUCTION

β-Glucosidase (EC 3.2.1.21) hydrolyzes β-glucosides at the non-reducing end of substrates and releases β-D-glucose. The enzyme also catalyzes the reverse reaction of the hydrolysis (condensation) and transglucosylation to produce new glycosidic linkages (Crout and Vic 1998). According to the sequence-based classification of glycoside hydrolases (Drula *et al*. 2022), β-glucosidases are classified into glycoside hydrolase family (GH) 1, GH2, GH3, GH5, GH16, GH30, GH39, GH116 and GH131 of the CAZy database. Among these families, GH3 contains β-glucosidases from bacteria, fungi, and plants. A representative GH3 β-glucosidase is barley HvExoI, which acts on various β-glucosides, such as β-glucans, aryl β-glucopyranosides, and β-glucooligosaccharides (Hrmova and Fincher 1997). GH3 β-glucosidases from filamentous fungi such as *Aspergillus* and *Trichoderma* have been also well studied as key enzymes in biomass degradation. They also act on a wide variety of substrates. Some GH3 β-glucosidases from plant pathogenic fungi are known to be involved in their pathogenicity. For example, plant antifungal saponins such as avenacin and α-tomatine undergo enzymatic hydrolysis to release their terminal D-glucose moieties resulting in reduction of their antifungal toxicity (Bowyer *et al*. 1995; Sandrock *et al*. 1995). Some are involved in degradation of plant cell walls (Walton 1994). β-glucosidases MoCel3A and MoCel3B from the rice blast fungus *Magnaporthe oryzae* cooperate with endoglucanases to degrade plant cell wall polysaccharides, namely cellulose, β1-3/1-4-glucan, and β1-3-glucan (Takahashi *et al*. 2011). Recombinantly produced β-glucosidase UeBgl3A from the smut fungus, *Ustilago esculenta,* also showed hydrolytic activity on barley β1-3/1-4-glucan in addition to β1-3- and 1-4-linked disaccharides (Nakajima *et al*. 2012).

Several three-dimensional structures of fungal GH3 β-glucosidases, such as

Aspergillus aculeatus AaBGL1 (Suzuki *et al*. 2013), *A. fumigatus* AfβG, *A. oryzae* AoβG (Agirre *et al*. 2016), *Hypocrea jecorina* HjCel3A (Karkehabadi *et al*. 2014), and *Neurospora crassa* NcCel3A (Karkehabadi *et al*. 2018), have been determined. They are mainly comprised of three domains, which are a $(\beta/\alpha)_8$-barrel-like domain, an α/β sandwich domain, and a fibronectin type Ⅲ-like domain. Their active sites are formed in the interface of the first and second domains, as observed in barley HvExoI (Varghese *et al*. 1999; Suzuki *et al*. 2013). Subsite −1 residues Asp92, Arg156, Lys189, His190, Tyr248, nucleophilic catalyst Asp280, Trp281, Ser451, and acid/base catalyst Glu509 (AaBGL1 numbering) are conserved and have hydrogen bonding and stacking interactions with the glucosyl moiety of substrates. In contrast, subsite +1 of most fungal GH3 β-glucosidases are formed by some less-conserved aromatic residues, e.g. Trp68, Phe305, and Tyr511 in AaBGL1 (Suzuki *et al*. 2013; Karkehabadi *et al*. 2014; Karkehabadi *et al*. 2018). The aforementioned broad substrate specificity of GH3 β-glucosidases is attributed to the subsite +1 structure.

Microdochium nivale is a phytopathogenic ascomycete found in cool and temperate regions worldwide that infects grasses and cereals (Hoshino *et al.* 2009, Tronsmo *et al.* 2001). Under snow cover, it infects host plants, causing pink snow mold (Jamalainen 1974); under cool and humid conditions in the absence of snow, it may also cause fusarium patch on grasses (Tronsmo *et al.* 2001), and is among the causal agents of fusarium head blight of cereals (Mesterházy *et al*. 2005). Isolates of *M. nivale* with high pathogenicity displayed higher extracellular β-glucosidase activity when they were grown with ryegrass cell wall as their carbon source (Hofgaard *et al*. 2006). Although the results suggest the involvement of GH3 β-glucosidase in fungal growth and pathogenicity, the *M. nivale* β-glucosidase itself has not previously been investigated to clarify its enzymatic properties and its protein sequence. In this study, we identified *M.*

nivale GH3 β-glucosidase MnBG3A which is secreted into the surrounding medium, and describe the enzymatic function of its recombinant enzyme produced in *Komagataella pastoris* transformants.

MATERIALS AND METHODS

Purification of MnBG3A. M. nivale MCW222-7 was obtained from Dr. Fumihiro Terami (National Agriculture and Food Research Organization [NARO], Hokkaido Agricultural Research Center, Sapporo, Japan). The hyphae of *M. nivale* MCW222-7, grown on potato dextrose (PD) agar medium (Becton, Dickinson and Company, Franklin Lakes, NJ, USA) at 4°C for 1 week, were cultured in 3 L of PD broth with vigorous shaking at 18°C for 4 weeks. The culture supernatant (2.6 L), obtained by centrifugation (6,000 ×*g*, 10 min, 4°C), was loaded onto a DEAE Sepharose Fast Flow column (Cytiva, Tokyo, Japan; 5.0 cm I.D. × 26 cm) equilibrated with 10 mM sodium phosphate buffer (pH 6.4). After non-adsorbed protein was eluted with the same buffer, adsorbed protein was eluted with a linear gradient of 0–500 mM NaCl. Active fractions collected were separated with a Butyl Sepharose 4 Fast Flow column (Cytiva; 2.8 cm I.D. × 12 cm) equilibrated with 10 mM sodium phosphate buffer (pH 7.0) containing 1.2 M ammonium sulfate. After washing with the same buffer, adsorbed protein was eluted with a linear gradient of 1.2–0 M ammonium sulfate. The active fractions collected were concentrated to 4 mL by ultrafiltration using Amicon Ultra YM30 (molecular weight cut off, 30,000; Merck Millipore, Billerica, MA, USA), and loaded on a Sephacryl S-200 column (Cytiva; 1.5 cm I.D. × 98 cm), equilibrated with 10 mM sodium phosphate buffer (pH 7.0) containing 0.1 M NaCl. An active fraction was stored at 4°C until analysis.

N-terminal amino acid sequence analysis. Purified MnBG3A (4.4 μg) was transferred to polyvinylidene difluoride membrane (Immobilon-P, Merck Millipore) with Trans-Blot SD Semi-Dry Transfer Cell (Bio-Rad, Hercules, CA, USA) from the SDS-PAGE gel. The N-terminal amino acid sequence of the 94-kDa protein was analyzed by direct sequencing with Procise 492HT (Perkin Elmer, Waltham, MA, USA).

LC-MS/MS analysis of tryptic peptides from MnBG3A. MnBG3A (0.88 μg) was separated by SDS-PAGE, followed by in-gel digestion using the In Gel Tryptic Digestion kit (Thermo Fisher Scientific, Waltham, MA, USA). The peptides were purified using the Pierce C18 Spin column (Thermo Fisher Scientific), and analyzed with LC-MS/MS Paradigm MS2 (Michrom BioResources, Auburn, CA, USA) under the following conditions: column, Zaplous α Pep-C18 (0.1 mm I.D. × 150 mm; AMR, Tokyo, Japan); elution, 35–90% acetonitrile linear gradient in 0.1% (v/v) formic acid; flow rate, 0.6 μL/min; MS, LTQ-Orbitrap XL (Thermo Fisher Scientific). Data were processed using the search software Proteome Discoverer (Thermo Fisher Scientific).

Whole genome sequencing of M. nivale and identification of the MnBG3A coding sequence. Genomic DNA of *M. nivale* YKP21-4, which was obtained from Dr. Fumihiro Terami, was prepared using the Powersoil DNA isolation kit (Mo Bio, Carlsbad, CA, USA). Genomic DNA libraries were prepared with the Kapa HTP gDNA Library Kit and sequenced using the Illumina HiSeq 2000 platform (Génome Québec, Montréal, Canada), to generate 100-bp paired-end reads. Reads were assembled with a range of Kmers (49–91), using three different programs: ABySS (Simpson *et al*. 2009), SOAP (Li *et al*. 2008), and Velvet (Zerbino *et al*. 2008). After discarding scaffolds less than 100 bp long, the assembly with the highest N50 value was kept for further analysis.

An annotated sequence data set (mn 13408) was created from the scaffolds using Augustus ver 3.0.2 (http://bioinf.uni-greifswald.de/augustus) based on the *Fusarium graminearum* gene model. To isolate a candidate gene for MnBG3A, a tblastn search of the mn13408 data set was carried out for N-terminal amino acid sequence of matured protein.

Construction of MnBG3A expression plasmid. From *M. nivale* cells grown at 18°C for 4 weeks, total RNA was prepared with TRIzol reagent (Thermo Fisher Scientific), and treatment with DNase I (Takara Bio, Kusatsu, Japan). cDNA was synthesized using Superscript III First-Strand Synthesis System for RT-PCR (Invitrogen, Carlsbad, CA, USA). The cDNA of MnBG3A was amplified by PCR using primers (5′-ATGCGCGCAACCTCGATCGC-3′, sense, and 5′-CTTGAGGTCAGCGCTGAGGG-3′, antisense) and KOD FX DNA polymerase (Toyobo, Osaka, Japan). The amplified DNA fragment was inserted into the site between the α-factor signal sequence and *c-myc* epitope sequence of pPICZαA (Invitrogen) using the In-Fusion HD Cloning Kit (Takara Bio) according to the manufacturer's method. The cloned DNA was sequenced using an Applied Biosystems 3130 Genetic Analyzer (Applied Biosystems, Foster City, CA, USA).

Preparation of recombinant MnBG3A. The pPICZαA derivative for the MnBG3A production was linearized at the *Pme*I site, and used for transformation of *K. pastoris* X-33 by electroporation using a Gene Pulser (Bio-Rad). Transformants were screened on YPDS agar plates (10 g/L yeast extract [Nacalai Tesque, Kyoto, Japan], 20 g/L peptone [Becton, Dickinson and Company], 20 g/L D-glucose, and 1 M D-glucitol) containing 100 mg/L zeocin. The transformant was grown in 400 mL of BMGY medium (10 g/L

yeast extract, 20 g/L peptone, 13.4 g/L yeast nitrogen base [Thermo Fisher Scientific], 4 mg/L biotin, 10 g/L glycerol, and 0.1 M potassium phosphate buffer [pH 6.0]) at 30°C with vigorous shaking for 16 hours, and subsequently cultured in 2 L of BMMY medium (as BMGY, but with 1% v/v methanol replacing glycerol) at 30°C for 144 h. Methanol (20 mL) was added every 24 h. Proteins in the culture supernatant (1.8 L) were precipitated with a 90%-saturation solution of ammonium sulfate, and dissolved in 500 mL of 10 mM sodium phosphate buffer (pH 7.0). The sample was subjected to chromatography on a Butyl Toyopearl 650M column (Tosoh, Tokyo, Japan; 2.8 cm I.D. × 24 cm) using buffer containing 1.2 M ammonium sulfate as a mobile phase. Active non-adsorbed fractions were collected and subjected to the same chromatography but using a mobile phase containing 1.6 M ammonium sulfate. Active proteins eluted with a decreasing linear gradient of ammonium sulfate concentration were collected. After dialysis against 10 mM sodium phosphate buffer (pH 7.0), DEAE Sepharose Fast Flow column chromatography was performed as for the native enzyme. The pooled fractions were dialyzed against 10 mM sodium phosphate buffer (pH 7.0), concentrated by Amicon Ultra YM30, and stored at 4°C until analysis.

Protein assay. Protein concentration in the purification procedures was determined by A_{280} under the assumption that the extinction coefficient of a 1 mg/mL of protein solution is 1. The concentration of the purified recombinant MnBG3A was measured by amino acid analysis using a high-speed amino acid analyzer (L-8900; Hitachi, Tokyo, Japan) after complete hydrolysis of the sample in 6 M HCl at 110°C for 24 h. The molecular masses of the subunit and MnBG3A in solution were determined by SDS-PAGE and blue native PAGE (Schägger *et al*. 1994), respectively. For the latter, the Native PAGE Sample Prep Kit (Life Technologies, Carlsbad, CA, USA) and Native

PAGE Novex 4–16% Bis-Tris Gels (Life Technologies) were used according to the manufacturer's instructions. Deglycosylated recombinant MnBG3A was prepared by heat denaturation of MnBG3A (0.42 μg) in 105 μL of 20 mM sodium acetate buffer (pH 5.0) at 100°C for 3 min, followed by incubation with 25 mU endoglycosidase H (Roche Diagnostics, Indianapolis, IN, USA) at 37°C for 18 h.

Standard enzyme assay. The reaction mixture (50 μL), consisting of 1 mM *p*-nitrophenyl β-D-glucoside (pNP-Glc, Tokyo Chemical Industry, Tokyo, Japan), 40 mM sodium acetate buffer (pH 4.6), 0.2 mg/mL bovine serum albumin (BSA) and an appropriate concentration of enzyme, was incubated at 30°C for 10 min. The enzyme reaction was terminated by adding 100 μL of 1 M Na_2CO_3, and liberated *p*-nitrophenol (pNP) was quantified based on A_{400}. Under these conditions, 1 U of enzyme was defined as the enzyme amount that produces 1 μmol of pNP in 1 min.

Effects of pH and temperature. The optimum pH was determined the same way as the standard activity assay, but the reaction buffer was replaced by 80 mM Britton-Robinson buffer with pH values ranging between 2.0 to 10.0 adjusted by titrating a mixture of phosphoric acid, acetic acid, and glycine (80 mM each) with 0.5 M sodium hydroxide. The optimum temperature was measured as for activity but using temperature ranges between 10 to 70°C. For pH stability, the enzyme (19.2 nM) was kept in 25 mM Britton-Robinson buffer (pH 2.0–12.0) at 4°C for 24 h, and residual activity was measured. For the thermal stability, the enzyme (1.92 nM) in 67 mM sodium acetate buffer (pH 4.6) was kept at 30–55°C for 15 min. Three independent replications of each experiment were conducted.

Glycone specificity. pNP β-D-fucopyranoside (pNP-Fuc, Sigma, St. Louis, MO, USA), pNP β-D-galactopyranoside (pNP-Gal, Sigma), pNP-Glc, pNP β-D-mannopyranoside (pNP-Man, Sigma), and pNP β-D-xylopyranoside (pNP-Xyl, Sigma) were used as substrates for recombinant MnBG3A. The enzyme concentration was 1.92 nM for pNP-Glc and 192 nM for the other substrates. The reaction conditions were the same as the standard enzyme assay, but with 2 mM substrate and pH 5.0. Three independent replications of each experiment were conducted.

Kinetic analysis of the reaction with pNP-Glc. The velocities for pNP- and D-glucose-release were measured in a reaction mixture (250 µL) consisting of 0.05–5 mM pNP-Glc, 40 mM sodium acetate buffer (pH 5.0), 0.2 mg/mL BSA and 0.192 nM MnBG3A at 30°C. pNP was quantified by measuring A_{400} after reaction aliquots (100 µL) were mixed with 50 µL of 2 M Na_2CO_3. D-Glucose was quantified with a Glucose CII Test (Fujifilm Wako Pure Chemical) (Huggett and Nixon 1957; Miwa *et al*. 1972) after aliquots (100 µL) were mixed with 50 µL of 4 M Tris-HCl buffer (pH 7.0). The substrate inhibition of pNP-releasing rates (Fig. 1a) was analyzed through regression with the rate equation (Eq. 1) by the Gauss-Newton method using R version 3.3.1 (Ihaka and Gentleman 1996).

Eq. 1 $$v/e_0 = k_{cat}\,[S]/([S]^2 / K_{is} + [S] + K_m)$$

where $k_{cat} = k_{+2}$, $K_m = (k_{-1} + k_{+2})/k_{+1}$, and $K_{is} = k_{-3}/k_{+3}$

Inhibition of the pNP releasing velocity by D-glucose was analyzed using the same reaction conditions, but with 0.1–2 mM pNP-Glc and 0–50 mM D-glucose. Equations 2 and 3, theoretically obtained from the reaction schemes according to the steady-state kinetic models 2 and 3 (Fig. 1c and d), respectively, were used for the regression.

Eq. 2 $$v/e_0 = k_{cat}\,[S] / ([S]^2/K_{is} + [S] + K_m[G]/K_i + K_m)$$

Eq. 3 $v/e_0 = k_{cat}[S] / ([S]^2/K_{is} + [S] + [G][S]/K_{i2} + K_m)$

where [S] and [G] are substrate and D-glucose concentrations, respectively. Kinetic parameters k_{cat}, K_m, and K_{is} are the same as defined above. K_i and K_{i2} are k_{-4}/k_{+4} and k_{-5}/k_{+5}, respectively. Three independent replications of each experiment were conducted.

Kinetic analysis for the hydrolysis of β-glucooligosaccharides. Reaction rates for sophorose (Sop_2, Sigma), laminarioligosaccharides (DP2−5; Lam_2–Lam_5, Megazyme, Bray, Ireland), cellobiose (Cel_2, Sigma), cellotriose (Cel_3, Megazyme), cellotetraose (Cel_4, Megazyme), and gentiobiose (Gen_2, Nacalai Tesque) were measured. For each substrate, a reaction mixture (100 μL) consisting of 0.08–0.8 mM substrate, 40 mM sodium acetate buffer (pH 5.0), 0.2 mg/mL BSA, and MnBG3A (1.92 nM for Sop_2 and 0.192 nM for the others) was incubated at 30°C for 10 min. Liberated D-glucose was measured as described above. For the disaccharide reaction rates, half of the glucose-release rates were used. Nonlinear regression with the Michaelis-Menten equation on [S] – v plots was done using Grafit version 7 (Erithacus Software, West Sussex, UK). Three independent replications of each experiment were conducted.

Transglucosylation with Gen_2 and Lam_2. A reaction mixture (50 μL) containing 20 mM Gen_2 or Lam_2, 40 mM sodium acetate buffer (pH 5.0), and 19.2 nM MnBG3A was incubated at 30°C. Aliquots (10 μL) were taken at 10, 30, 60, and 120 mins (Gen_2) or 3, 6, 9, 20, and 30 mins (Lam_2), and kept at 100°C for 3 min to terminate the reaction. One μL of each reaction solution was analyzed by TLC using a Silica gel 60 F_{254} plate (Merck, Darmstadt, Germany) developed in 2-propanol:1-butanol:water 12:3:4 and 2:2:1 (v/v) for the products from Gen_2 and Lam_2, respectively, followed by detection

with acetic acid:sulfuric acid:anisaldehyde 100:2:1 (v/v). The solution was reacted with Lam_2 for 30 min in the same conditions and was analyzed by high-performance anion-exchange chromatography with pulsed amperometric detection (HPAEC-PAD) using CarboPac PA-1 (4 mm I.D. × 250 mm; Thermo Fischer Scientific) with linear gradient of 0–250 mM sodium acetate with isocratic 0.4 M NaOH at 0.8 mL/min.

Condensation of D-glucose. A reaction mixture (100 μL) consisting of 2.1 M D-glucose, 10 mM sodium phosphate buffer (pH 7.0), and 9.6 μM MnBG3A was incubated at 30°C for 4 days. The reaction was terminated by heating the sample at 100°C for 3 min. Sugar composition was analyzed by TLC as described above, and by HPAEC-PAD with isocratic 0.4 M NaOH at 0.8 mL/min.

RESULTS

Identification of extracellular β-glucosidase MnBG3A from M. nivale. A 3-L flask fermentation of *M. nivale* in PD broth without additional inducer for 4 weeks at 18°C yielded 111 U of β-glucosidase in the culture supernatant. The enzyme MnBG3A was purified by three types of column chromatography: anion-exchange, hydrophobic interaction, and gel permeation. The activity was not separated, and eluted in a single peak. The purified protein (0.110 mg, 0.83 U) showed specific activity of 7.57 U/mg and an almost single band at 111 kDa on SDS-PAGE analysis (Fig. 2a). Partial amino acid sequences of MnBG3A obtained by N-terminal sequencing by Edman degradation and liquid chromatography-tandem mass spectrometry (LC-MS/MS) analysis of tryptic peptides was used to pull out a candidate gene for MnBG3A from *M. nivale* genome sequence data. The 11 residues determined by the N-terminal sequencing were identical to Ala32–Val42 of the deduced amino acid sequence. The MS/MS spectra of the tryptic

peptides closely matched the deduced sequence with 46% coverage of the entire protein sequence deduced from the cDNA sequence. The sequence of the MnBG3A-coding DNA is deposited in the DDBJ database under accession number LC723725.

The deduced protein sequence indicates that MnBG3A is an 845-residue protein (Ala32–K876) of theoretical molecular weight of 91,212, after the removal of Met1–Arg31 of the immature protein. It contains 10 possible *N*-glycosylation sites. A BLASTp search against non-redundant protein sequences revealed that MnBG3A is a GH3 protein with the highest identity (91%) to putative GH3 β-glucosidase A derived from *Microdochium bolleyi* (NCBI ID KXJ94594.1). A high identity (60%) was also observed with well-characterized GH3 β-glucosidase AaBGL1 from *Aspergillus aculeatus* (Takada *et al*. 1998). In addition to the overall similarity, the essential residues conserved in the fungal GH3 enzymes were found in the MnBG3A sequence (Fig. 3): i.e. the catalytic nucleophile (Asp295), the general acid/base (Glu523), and amino acid residues involved in subsite −1 (Asp107, Arg171, Lys204, His205, Tyr263, Trp296, and Ser464). The subsite +1 residues having hydrophobic interaction with substrate in AaBGL1 (Trp83, Phe320, and Tyr525) were also found in MnBG3A.

Recombinant MnBG3A produced in K. pastoris. Recombinant MnBG3A (1,150 U) was produced in the 2-L culture supernatant after 144-h culture at 20°C by the *K. pastoris* transformant harboring a gene encoding the mature MnBG3A (Ala32–Lys876) with the plasmid-derived signal sequence of α-factor attached at the N-terminus. The enzyme (320 U, 7.04 mg) was purified by ammonium sulfate precipitation and column chromatography. Specific activity of the recombinant MnBG3A (45.5 U/mg) was 6-fold higher than that of the native enzyme, possibly because of the low purity of the native enzyme. The purified enzyme showed a clear single band at 129 kDa on SDS-PAGE

(Fig. 2b) and at 256 kDa on blue native PAGE (Fig. 2c). Digestion with endoglycosidase H decreased the molecular mass to 98 kDa on SDS-PAGE, which was close to the theoretical mass from the amino acid sequence of 92 kDa (Fig. 2b). These data suggest that recombinant MnBG3A was *N*-glycosylated, and existed as dimer in solution. Recombinant MnBG3A showed the highest activity at pH 5.1 and 50°C (Fig. 4). The enzyme activity was ≥90% retained after incubation at pH values ranging between 5.1 to 10.0 (4°C for 24 h) and at temperatures ≤40°C (for 15 min) (Fig. 4).

Substrate specificity. The pNP-releasing velocity with 2 mM pNP β-glycosides (pNP-Glc, pNP-Man, pNP-Gal, pNP-Xyl, and pNP-Fuc) was measured. Recombinant MnBG3A acted only upon pNP-Glc and pNP-Xyl at reaction rates of 50.4 ± 1.9 s^{-1} and 0.200 ± 0.001 s^{-1}, respectively. The velocity for the other glycosides was not detectable (<0.0076 s^{-1}). In the reaction to pNP-Glc, pNP- and glucose-releasing velocities were almost identical at 0.05–5 mM concentrations of the substrate (Fig. 5a), indicating that MnBG3A catalyzed hydrolysis and no detectable transglycosylation under the conditions. However, a severe decrease in velocity was observed in a higher range of substrate, particularly over 0.3 mM. The rate equation for the substrate inhibition (Fig. 1a, Eq. 1) was well fitted to the reaction rates with the following kinetic parameters: k_{cat}, 112 ± 4 s^{-1}; K_m, 0.0841 ± 0.0035 mM; and K_{is} (ESS-dissociation constant), 1.61 ± 0.13 mM. The result also supports the reaction scheme involving the formation of the glucosyl enzyme intermediate and pNP-Glc complex (Fig. 1b), which raises the same equation (Eq. 1), although the parameters k_{cat}, K_{is}, and K_m are expressed as a combination of different rate constants. The reaction of MnBG3A with pNP-Glc was inhibited also by D-glucose in a concentration-dependent manner (Fig. 5b). Two possible inhibition models involving the binding of D-glucose to free enzyme

(competitive inhibition) (Fig. 1c) and to the ES complex (uncompetitive inhibition) (Fig. 1d) were examined. The regression analysis indicated that the inhibition by D-glucose was competitive with kinetic parameters of k_{cat}, 105 ± 7 s^{-1}; K_m, 0.0786 ± 0.0104 mM; K_{is}, 2.01 ± 0.41 mM; and K_i (E Glc-dissociation constant), 0.491 ± 0.016 mM. The k_{cat}, K_m, and K_{is} determined were consistent with the values from the reactions in the absence of D-glucose.

MnBG3A also hydrolyzed various β-glucooligosaccharides (Table 1). The reactions obeyed Michaelis-Menten kinetics in the substrate concentration range of 0.08–0.8 mM. Of the glucobioses tested, β1-3-linked Lam_2 showed the highest k_{cat}/K_m ratio (1,410 $s^{-1}mM^{-1}$) followed by Gen_2 (β1-6, 720 $s^{-1}mM^{-1}$), Cel_2 (β1-4, 179 $s^{-1}mM^{-1}$), and Sop_2 (β1-2, 56.4 $s^{-1}mM^{-1}$) (Table 1). The trisaccharide Lam_3 showed the highest k_{cat}/K_m of laminarioligosaccharides, whereas the highest k_{cat}/K_m among the cellooligosaccharides was observed for the longest oligosaccharide (Cel_4) tested.

Transglucosylation and condensation. MnBG3A was incubated with Gen_2 and Lam_2 at 20 mM, much higher than the concentrations used in the kinetic analysis, and the products were analyzed by TLC (Fig. 6a and b). In the reaction with Gen_2, gentiotriose (Gen_3) along with D-glucose were detected as products (Fig. 6a). In the reaction with Lam_2, Gen_2 and D-glucose were predominantly produced with trace quantities of Lam_3 detected (Fig. 6b). This suggests that D-glucose, produced by hydrolysis in the early stage, served as acceptor of the transglucosylation. Therefore, transglucosylation of MnBG3A uses mainly Gen_2 and D-glucose as acceptors, and forms predominantly β1-6 linkages. MnBG3A was also incubated with 2.1 M D-glucose as the sole substrate for a longer time to analyze the condensation. Both the TLC and HPAEC-PAD analyses indicated predominant production of Gen_2 (Fig. 6c and d). In the HPAEC-PAD

chromatogram, peaks at 5.1 and 5.8 min of retention time corresponded to Sop_2 or Lam_2 and Gen_3, respectively (Fig. 6d). Quantification with the HPAEC-PAD indicated that Gen_2 reached a concentration of 89.5 mM in 4 days. The conversion ratio was 8.5% of the total conversion on a molar basis, and the equilibrium constant $K_{eq} = [Gen_2]/[Glc]$ was 0.047. The results of condensation also indicate that MnBG3A is highly β1-6 linkage specific in the formation of glycosidic linkages.

DISCUSSION

Microdochium nivale is a phytopathogenic filamentous fungus that causes pink snow mold, fusarium patch, and fusarium head blight in gramineous plants. Although the involvement of β-glucosidase in its growth and pathogenicity was previously suggested (Hofgaard *et al*. 2006), little is known about *M. nivale* β-glucosidase itself. In this study, a GH3 enzyme, extracellular β-glucosidase MnBG3A, was identified and characterized mainly using recombinant enzyme produced in a *K. pastoris* transformant. The sequence comparison indicated that MnBG3A is 91% identical to putative GH3 β-glucosidase A derived from *M. bolleyi* and 60% identical to AaBGL1, one of the most well-studied fungal GH3 β-glucosidase in terms of its function and structure. MnBG3A was very similar to AaBGL1 in its enzymatic functions, particularly substrate specificity to various pNP β-glycosides and β-glucobioses, and in terms of its chain length preferences for cellooligosaccharides and laminarioligosaccharides (Baba *et al*. 2015). These functional similarities are explained by the high structural similarity, particularly the highly conserved subsites −1 and +1-forming residues as shown in the multiple sequence alignment (Fig. 3).

Differences between MnBG3A and AaBGL1 were observed in terms of the inhibition of MnBG3A by both the substrate and product in reactions with pNP-Glc.

MnBG3A was inhibited by pNP-Glc with a K_{is} value of 1.6 mM, but AaBGL1 followed Michaelis-Menten equation with 0.1–1.2 mM pNP-Glc, and substrate inhibition was not observed (Suzuki *et al*. 2013). Higher inhibition by D-glucose was also exhibited by MnBG3A. The K_i value is significantly lower in MnBG3A (0.491 mM) than AaBGL1 (K_i 9.99 mM; Baba *et al*. 2015). Taken together, MnBG3A is more sensitive than AaBGL1 in exhibiting inhibitory effects by both pNP-Glc and D-glucose.

Inhibition by both substrate and product have been reported in some fungal GH3 β-glucosidases. In *Penicillium brasilianum* BGL and *A. oryzae* AoCel3, substrate and product inhibitions were observed with K_i values to D-glucose of 2.3 and 2.9 mM, respectively (Krogh *et al*. 2010; Langston *et al*. 2006). However, the decline of the pNP-generating rates at a higher range of pNP-Glc concentrations in the AoCel3A-catalyzing reaction was clearly explained by transglucosylation kinetics (Langston *et al*. 2006). Before this report, a similar rate decrease in Lam_2 hydrolysis by a GH3 β-glucosidase of the white-rot fungus *Phanerochaete chrysosporium* was clearly demonstrated to follow the hydrolysis-transglucosylation reaction scheme (Kawai *et al*. 2004). In the reaction scheme, after the formation of the glucosyl enzyme intermediate through the cleavage of substrate, water and substrate are bound to the intermediate in a competitive manner. Therefore, the higher concentration of substrate gives higher transglucosylation, but if the rate constant for the synthesis of the transglucosylation product from the glucosyl enzyme-substrate complex is low, the overall reaction rate decreases with increasing substrate concentration as mentioned above for the GH3 β-glucosidases. When this rate constant is zero, the reaction scheme is as shown in Fig. 1b and gives the same inhibition equation (Eq. 1). Considering the similarity of all of the GH3 β-glucosidases, the substrate inhibition of MnBG3A occurs probably not via simple ESS formation, but rather the formation of the glucosyl enzyme intermediate and

pNP-Glc complex. The second pNP-Glc binds at subsites +1 and +2 of the glucosyl enzyme intermediate, as it binds as an acceptor molecule in transglucosylation, but in a non-productive manner in MnBG3A.

MnBG3A catalyzed β1-6 transglucosylation using D-glucose and Gen_2 as acceptors. Gen_2 was also produced in the condensation reaction. As for AaBGL1, transglucosylation and condensation were not thoroughly analyzed, but Gen_2 was detected in small amounts in the reaction with 25 mM Cel_2 or Lam_2 (Baba *et al*. 2015). The generation of β1-6 linkages through transglucosylation was also reported in several other fungal GH3 β-glucosidases. In the transglucosylation of Cel_2 by AnBGL, 6^{II}-*O*-β-D-glucosyl cellobiose was produced initially, followed by Gen_2 after accumulation of D-glucose in concentrations over 5 mM (Seidle and Huber 2005). In the reaction of Lam_2 by *Penicillium chrysosporium* PcBgl1A, only 6^{II}-*O*-β-D-glucosyl laminaribiose was generated as the transglucosylation product (Kawai *et al*. 2004). The β1-6 linkage formation is shared by all the reactions, but acceptor preferences to D-glucose and the disaccharides are different. The different acceptor preferences suggest structural differences in subsite +2. In MnBG3A, binding of the reducing-end D-glucosyl moiety of Gen_2 in subsite +2 was suitable for the nonreducing-end D-glucosyl moiety to bind in subsite +1 for the formation of β1-6 linkages. The binding of Lam_2 in subsite +2, however, placed the nonreducing-end D-glucosyl moiety in an orientation not suitable for the linkage formation. The inhibition and transglucosylation with pNP-Glc mentioned above also support the difference in subsite +2 of MnBG3A compared to the other enzymes. No complex structure indicating subsite +2 has been determined yet, which makes it difficult to predict which residues are involved in the activity at this subsite.

As observed in AaBGL1, MnBG3A has higher β1-3 linkage specificity in

hydrolysis though it has broad substrate specificity. The substrate preference of MnBG3A is suitable for its involvement in degradation of cellulose through Cel_2 hydrolysis, and also in degradation of hemicellulosic β1-3-glucan and β1-3/1-4-glucan, as mentioned for the *Magnaporthe oryzae* GH3 β-glucosidases, MoCel3A and MoCel3B (Takahashi *et al*. 2011). *Microdochium bolleyi*, which encodes a putative enzyme with the highest identity to MnBG3A identified in a BLASTp search, is generally known as an endophyte of grasses and grows in root cells of healthy plants (David *et al*. 2016). Its GH3 β-glucosidase A is probably required for plant cell invasion and proliferation of the fungus. The broad substrate specificity of MnBG3A is suitable for these physiological roles. In addition, the transglucosylation activity of MnBG3A implies that another possible role of MnBG3A is Gen_2 production, which is an inducer of cellulolytic enzymes in *Penicillium purpurogenum* (Kurasawa *et al*. 1992; Suto and Tomita 2001). This would be beneficial for plant infection and the proliferation of *M. nivale*.

In summary, *M. nivale* was shown to possess the GH3 β-glucosidase MnBG3A, which has similar characteristics to fungal GH3 β-glucosidases but with higher sensitivity to inhibitory effects. From the perspective that this fungus is phytopathogenic, this enzyme is considered to act on β-glucooligosaccharides generated from cellulose and/or hemicelluloses by β-glucanases. In addition, MnBG3A might be involved in the induction of cellulases through the production of a possible inducer, Gen_2, by transglucosylation in *M. nivale.*

Conflicts of interest:

The authors declare that there is no conflict of interest.

Acknowledgments:

We are grateful to Seiko Oka, Nozomi Takeda, and Tomohiro Hirose of the Instrumental Analysis Division, Global Facility Center, Creative Research Institution, Hokkaido University for protein identification analysis, amino acid analysis and N-terminal amino acid sequence analysis. We thank the staff of the DNA Sequencing Facility of the Research Faculty of Agriculture, Hokkaido University for assistance with DNA sequence analyses.

Funding:

This work was partly supported by the Hokkaido University Ambitious Doctoral Fellowship (SDGs).

Author contributions:

T.O. conceived and designed the experiments, performed the biochemical experiments, and wrote the paper. W.S. conceived and designed the experiments, performed the biochemical experiments, and wrote the paper. L.J. and T.H. performed whole genome sequencing of *M. nivale* and wrote the paper. R.I. and H.M. conceived and designed the experiments and wrote the paper.

Data availability:

The data underlying this article will be shared upon reasonable request to the corresponding author.

<References>

Agirre J, Ariza A, Offen WA, Turkenburg JP, Roberts SM, Mcnicholas S, Harris PV, Mcbrayer B, Dohnalek J, Cowtan KD, Davies GJ, and Wilson KS. Three-dimensional structures of two heavily N-glycosylated *Aspergillus* sp. family GH3 β-D-glucosidases. *Acta Crystallogr D Struct Biol* 2016;**72**:254–265.

Baba Y, Sumitani J, Tani S, and Kawaguchi T. Characterization of *Aspergillus aculeatus* β-glucosidase 1 accelerating cellulose hydrolysis with *Trichoderma* cellulase system. *AMB Express* 2015;**5**:3.

Bowyer P, Clarke BR, Lunness P, Daniels MJ, and Osbourn AE. Host range of a plant pathogenic fungus determined by a saponin detoxifying enzyme. *Science* 1995;**267**:371–374.

Crout DH and Vic G. Glycosidases and glycosynthetases in glycoside and oligosaccharide synthesis. *Curr Opin Chem Biol* 1998;**2**:98–111.

David AS, Haridas S, LaButti K, Lim J, Lipzen A, Wang M, Barry K, Grigoriev IV, Spatafora JW, and May G. Draft genome sequence of *Microdochium bolleyi*, a dark septate fungal endophyte of beach grass. *Genome Announc* 2016;**4**:e00270-16.

Drula E, Garron ML, Dogan S, Lombard V, Henrissat B, and Terrapon N. The carbohydrate-active enzyme database: functions and literature. *Nucleic Acids Res* 2022;**50**:D571–D577.

Hofgaard IS, Wanner LA, Hageskal G, Henriksen B, Klemsdal SS, and Tronsmo AM. Isolates of *Microdochium nivale* and *M. majus* differentiated by pathogenicity on perennial ryegrass (*Lolium perenne* L.) and *in vitro* growth at low temperature. *J Phytopathol* 2006;**154**:267–274.

Hoshino T, Xiao N, and Tkachenko OB. Cold adaptation in the phytopathogenic fungi causing snow molds. *Mycoscience* 2009;**50**:26–38.

Hrmova M and Fincher GB. Barley β-D-glucan exohydrolases. Substrate specificity and kinetic properties. *Carbohydr Res* 1997;**305**:209–221.

Huggett ASG and Nixon DA. Use of glucose oxidase, peroxidase, and O-dianisidine in determination of blood and urinary glucose. *Lancet* 1957;**270**:368–370.

Ihaka R and Gentleman R. R: a language for data analysis and graphics. *J Comp Graph Stat* 1996;**5**:299–314. Available via http://www.R-project.org.

Jamalainen EA. Resistance in winter cereals and grasses to low-temperature parasitic fungi. *Annu Rev Phytopathol* 1974;**12**:281–302.

Karkehabadi S, Hansson H, Mikkelsen NE, and Kim S. Structural studies of a glycoside hydrolase family 3 β-glucosidase from the model fungus *Neurospora crassa*. *Acta Crystallogr F Struct Biol Commun* 2018;**74**:787–796.

Karkehabadi S, Helmich KE, Kaper T, Hansson H, Mikkelsen N, Gudmundsson M,

Piens K, Fujdala M, Banerjee G, Scott-Craig JS, Walton JD, Phillips Jr GN, and Sandgren M. Biochemical characterization and crystal structures of a fungal family 3 β-glucosidase, Cel3A from *Hypocrea jecorina. J Biol Chem* 2014;**289**:31624–31637.

Katoh K, Rozewicki J, and Yamada KD. MAFFT online service: multiple sequence alignment, interactive sequence choice and visualization. *Brief Bioinform* 2019;**20**:1160–1166. Available via https://mafft.cbrc.jp/alignment/server/.

Kawai R, Igarashi K, Kitaoka M, Ishii T, and Samejima M. Kinetics of substrate transglycosylation by glycoside hydrolase family 3 glucan (1→3)-β-glucosidase from the white-rot fungus *Phanerochaete chrysosporium*. *Carbohydr Res* 2004;**339**:2851–2857.

Krogh KBRM, Harris PV, Olsen CL, Johansen KS, Hojer-Pedersen J, Borjesson J, and Olsson L. Characterization and kinetic analysis of a thermostable GH3 beta-glucosidase from *Penicillium brasilianum*. *Appl Microbiol Biotechnol* 2010;**86**:143–154.

Kurasawa T, Yachi M, Suto M, Kamagata Y, Takao S, and Tomita F. Induction of cellulase by gentiobiose and its sulfur-containing analog in *Penicillium purpurogenum*. *Appl Environ Microbiol* 1992;**58**:106–110.

Langston J, Sheehy N, and Xu F. Substrate specificity of *Aspergillus oryzae* family 3 β-glucosidase. *Biochim Biophys Acta* 2006;**1764**:972–978.

Li R, Li Y, Kristiansen K, and Wang J. SOAP: short oligonucleotide alignment program.

Bioinformatics 2008;**24**:713–714.

Mesterházy Á, Bartók T, Kászonyi G, Varga M, Tóth B, and Varga J. Common resistance to different *Fusarium* spp. Causing *Fusarium* head blight in wheat. *Eur J Plant Pathol* 2005;**112**:267–281.

Miwa I, Okudo J, Maeda K, and Okuda G. Mutarotase effect on colorimetric determination of blood glucose with β-D-glucose oxidase. *Clin Chim Acta* 1972;**37**:538–540.

Nakajima M, Yamashita T, Takahashi M, Nakano Y, and Takeda T. Identification, cloning, and characterization of β-glucosidase from *Ustilago esculenta*. *Appl Microbiol Biotechnol* 2012;**93**:1989–1998.

Robert X and Gouet P. Deciphering key features in protein structures with the new ENDscript server. *Nucl Acids Res* 2014;**42**:W320–W324. Available via http://espript.ibcp.fr.

Sandrock RW, DellaPenna D, and VanEtten HD. Purification and characterization of β_2-tomatinase, an enzyme involved in the degradation of α-tomatine and isolation of the gene encoding β_2-tomatinase from *Septoria lycopersici*. *Mol Plant Microbe Interact* 1995;**8**:960–970.

Schägger H, Cramer WA, and von Jagow G. Analysis of molecular masses and oligomeric states of protein complexes by blue native electrophoresis and isolation of

membrane protein complexes by two-dimensional native electrophoresis. *Anal Biochem* 1994;**217**:220–230.

Seidle HF and Huber RE. Transglucosidic reactions of the *Aspergillus niger* family 3 β-glucosidase: Qualitative and quantitative analyses and evidence that the transglucosidic rate is independent of pH. *Arch Biochem Biophys* 2005;**436**:254–264.

Simpson JT, Wong K, Jackman SD, Schein JE, Jones SJ, and Birol I. AbySS: a parallel assembler for short read sequence data. *Genome Res* 2009;**19**:1117–1123.

Suto M and Tomita F. Induction and catabolite repression mechanisms of cellulase in fungi. *J Biosci Bioeng* 2001;**92**:305–311.

Suzuki K, Sumitani JI, Nam YW, Nishimaki T, Tani S, Wakagi T, Kawaguchi T, and Fushinobu S. Crystal structures of glycoside hydrolase family 3 β-glucosidase 1 from *Aspergillus aculeatus*. *Biochem J* 2013;**452**:211–221.

Takahashi M, Konishi T, and Takeda T. Biochemical characterization of *Magnaporthe oryzae* β-glucosidases for efficient β-glucan hydrolysis. *Appl Microbiol Biotechnol* 2011;**91**:1073–1082.

Takada G, Kawaguchi T, Sumitani J, and Arai M. Expression of *Aspergillus aculeatus* No. F-50 cellobiohydrolase I (*cbhI*) and β-glucosidase 1 (*bgl1*) genes by *Saccharomyces cerevisiae*. *Biosci Biotechnol Biochem* 1998;**62**:1615–1618.

Tronsmo AM, Hsiang T, Okuyama H, and Nakajima T. Low temperature diseases caused by *Microdochium nivale*. In: Iriki N, Gaudet DA, Tronsmo AM, Matsumoto N, Yoshida M, Nishimune A (eds). Low temperature plant microbe interactions under snow. Hokkaido National Agricultural Experimental Station, 2001, 75–86.

Varghese JN, Hrmova M, and Fincher GB. Three-dimensional structure of a barley β-D-glucan exohydrolase, a family 3 glycosyl hydrolase. *Structure* 1999;**7**:179–190.

Walton JD. Deconstructing the cell wall. *Plant Physiol* 1994;**104**:1113–1118.

Zerbino D and Birney E. Velvet: algorithms for de novo short read assembly using de Bruijn graphs. *Genome Res* 2008;**18**:821–829.

Table 1. Kinetic parameters of recombinant MnBG3A

Substrate	k_{cat} (s^{-1})	K_m (mM)	k_{cat}/K_m ($s^{-1}mM^{-1}$)	K_{is} [c] (mM)	K_i [d] (mM)
pNP-Glc [a]	112 ± 4	0.0841 ± 0.0035	1330	1.61 ± 0.13	n.a.
pNP-Glc [b]	105 ± 7	0.0786 ± 0.0104	1350	2.01 ± 0.41	0.491 ± 0.016
Sophorose	80.1 ± 3.0	1.42 ± 0.07	56.4	n.a.	n.a.
Lainaribiose	133 ± 2	0.0951 ± 0.0092	1410	n.a.	n.a.
Laminaritriose	144 ± 7	0.0792 ± 0.0086	1830	n.a.	n.a.
Laminaritetraose	138 ± 6	0.108 ± 0.010	1290	n.a.	n.a.
Laminaripentaose	159 ± 3	0.292 ± 0.006	544	n.a.	n.a.
Cellobiose	67.0 ± 6.5	0.379 ± 0.063	179	n.a.	n.a.
Cellotriose	96.2 ± 4.1	0.104 ± 0.016	945	n.a.	n.a.
Cellotetraose	80.0 ± 2.2	0.0735 ± 0.0081	1090	n.a.	n.a.
Gentiobiose	136 ± 3	0.188 ± 0.008	720	n.a.	n.a.

a, parameters calculated from Eq. 1. b, parameters calculated from Eq. 3. n.a., not analyzed.

c, ESS-dissociation constant, referring to Fig. 1a. d, E Glc-dissociation constant, referring to Fig. 1b.

Graphical abstract caption:

MnBG3A has sensitivity to inhibitory effects, prefers laminaribiose in disaccharide hydrolysis, and generates β1-6 glucosidic linkages in transglucosylation.

Figure captions:

Fig. 1. Reaction schemes for hydrolysis of pNP-Glc

(a) the scheme of substrate inhibition of the simple ESS formation; (b) the scheme of substrate inhibition of the formation of the glucosyl enzyme intermediate and pNP-Glc complex; (c) the scheme of competitive inhibition by D-glucose; (d) the scheme of uncompetitive inhibition by D-glucose. “E”, enzyme; “S”, substrate; “ES”, ES complex; “ESS”, inactive complex of enzyme and two substrates; “E-Glc”, the glucosyl enzyme intermediate; “E-Glc S”, the glucosyl enzyme intermediate and substrate complex; “E Glc”, enzyme-D-glucose complex; “Glc”, D-glucose; “ES Glc”, ES-D-glucose complex.

Fig. 2. SDS-PAGE and blue native PAGE of purified native and recombinant MnBG3A

Purified MnBG3A (1.0 μg for SDS-PAGE and 5.0 μg for blue native PAGE) was analyzed. (a) SDS-PAGE of native MnBG3A; (b) SDS-PAGE of recombinant MnBG3A; (c) blue native PAGE of recombinant MnBG3A. Protein was stained with CBB. Lane M, size markers. Lane S, purified MnBG3A. Lane S1, purified MnBG3A. Lane S2, Endo H treated MnBG3A.

Fig. 3. Multiple alignment of partial amino acid sequences of MnBG3A and other fungal GH3 β-glucosidases

The amino acid sequence of AaBGL1, AnBGL, AoCel3, MnBG3A, and PcBgl1A were

aligned with MAFFT ver. 7 (Katoh *et al*. 2019; https://mafft.cbrc.jp/alignment/server/). The results of alignment were visualized using ESPript 3.0 (Robert and Gouet 2014; http://espript.ibcp.fr/). Circles and arrowheads indicate the residues at subsites −1 and +1, respectively. Square indicates catalytic nucleophile and star indicates catalytic acid base.

Fig. 4. Effects of pH and temperature on activity and stability of recombinant MnBG3A

Open and closed circles show activity and stability, respectively. (a) effect of pH on recombinant MnBG3A. Stability was evaluated by residual activity after incubation at 4°C for 24 h in the various pH conditions. (b) effect of temperature on recombinant MnBG3A. Stability was evaluated by residual activity after incubation for 15 min at the various temperatures. Values are average of the values from three independent experiments, and error bars indicate their standard deviation.

Fig. 5. *s*-*v* plot of MnBG3A for the hydrolysis of pNP-Glc

Values and error bars are mean and standard deviation for three independent experiments. (a) reaction with pNP-Glc. Closed circles, pNP-releasing velocity; open circles, Glc-releasing velocity; line, theoretical line for pNP release. (b) hydrolysis of pNP-Glc in the presence of various concentration of D-glucose. Closed circles, 0 mM; open circles, 2 mM; closed triangles, 10 mM; open triangles, 20 mM; closed squares, 50 mM; open squares, 100 mM. Theoretical lines from Eq. 2 (solid line) and Eq. 3 (dotted line) were fit to the experimental values.

Fig. 6. TLC and HPAEC-PAD analysis of MnBG3A reaction products from Gen_2,

Lam_2, and D-glucose

MnBG3A (19.2 nM) was incubated with 20 mM Gen_2 (a) and Lam_2 (b) for the indicated time and analyzed by TLC. MnBG3A (9.6 μM) was incubated with 2.1 M D-glucose for indicated time (c) and 4 days (d). Lane M1, Glc and laminarioligosaccharides; Lane M2, gentiooligosaccharides; Lane L, Lam_2; Lane G, Gen_2; Lane C, Cel_2; Lane S, Sop_2.

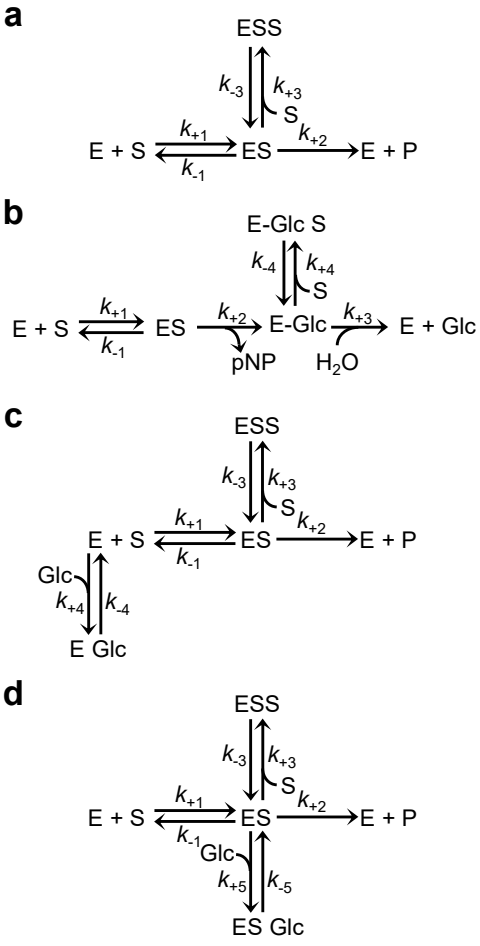

(Fig. 1, Ota *et al.*)

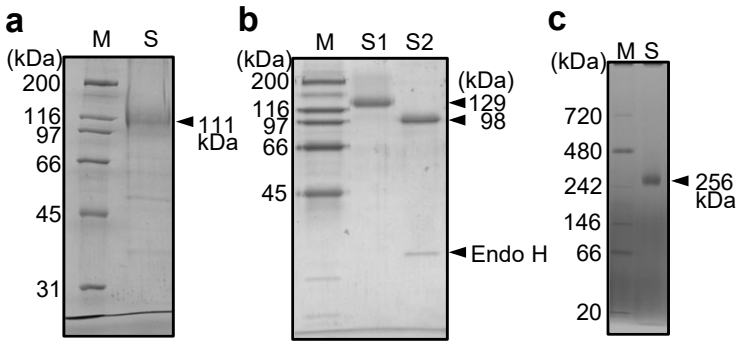

(Fig. 2, Ota *et al*.)

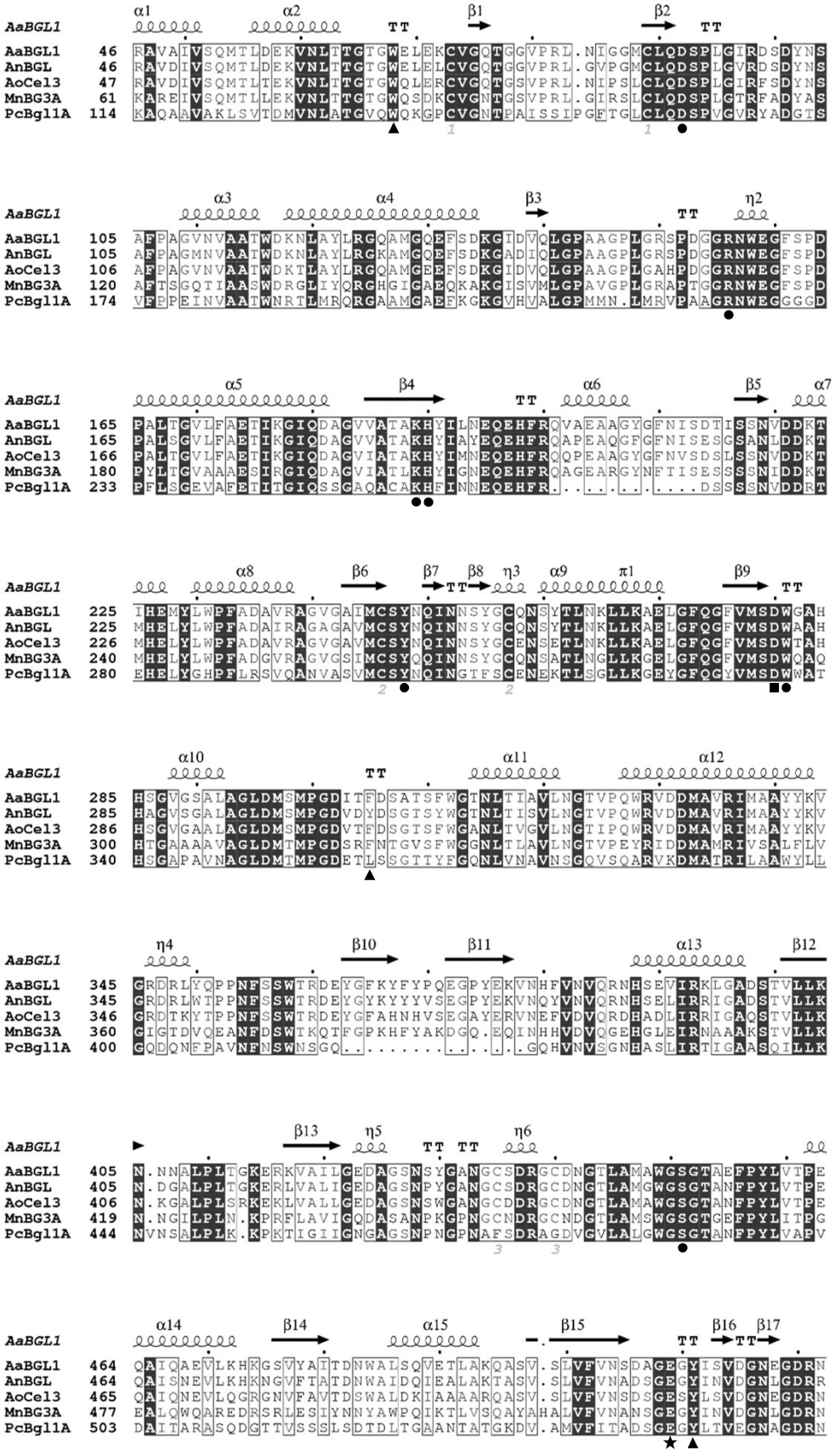

(Fig. 3, Ota *et al.*)

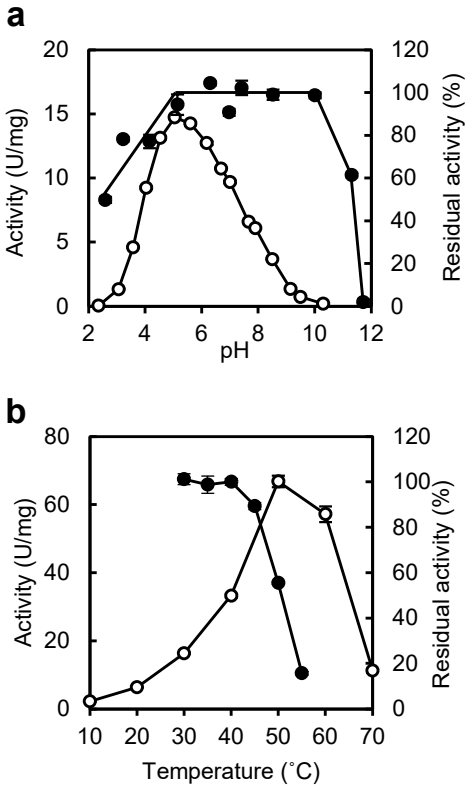

(Fig. 4, Ota *et al*.)

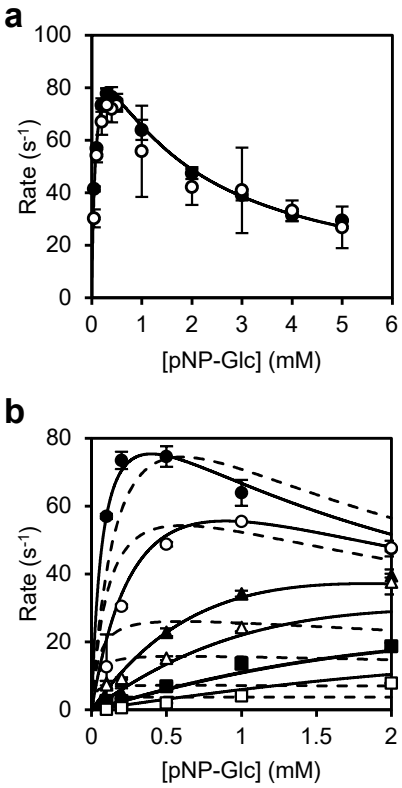

(Fig. 5, Ota *et al*.)

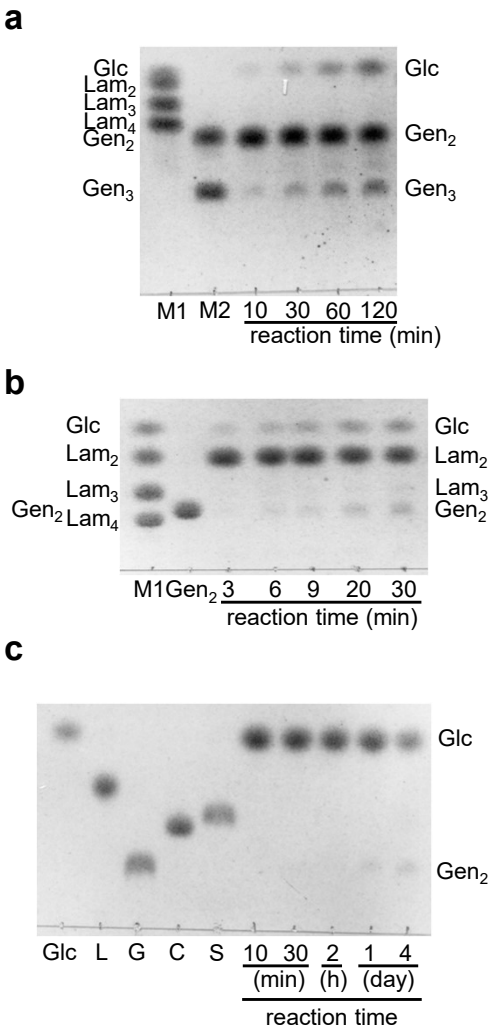

(Fig. 6, Ota *et al*.)